Low-temperature photoluminescence of CuSe$_2$ nano-objects in selenium thin films

Martina Gilić[1,*], Milica Petrović[1], Jovana Ćirković[2], Novica Paunović[1],
Svetlana Savić-Sević[1], Željka Nikitović[1], Maja Romčević[1], Ibrahim Yahia[3],
Nebojša Romčević[1]

[1]*Institute of Physics Belgrade, University of Belgrade, Pregrevica 118, Belgrade, Serbia*
[2]*The Institute for Multidisciplinary Research, University of Belgrade, Belgrade, Serbia*
[3]*Nano-Science and Semiconductors Labs., Physics Department, Faculty of Education, Ain Shams University, Roxy, Cairo, Egypt*

Abstract

Thin films of CuSe$_2$ nanoparticles embedded in selenium matrix were prepared by vacuum evaporation method on a glass substrate at room temperature. The optical properties of the films were investigated by photoluminescence spectroscopy (T = 20–300 K) and UV-VIS spectroscopy (T = 300 K). Surface morphology was investigated by scanning electron microscopy. The band gap for direct transition in CuSe$_2$ was found to be in the range of 2.72–2.75 eV and that for indirect transition is in the range of 1.71–1.75 eV determined by UV-VIS spectroscopy. On the other hand, selenium exhibits direct band gap in the range of 2.33–2.36 eV. All estimated band gaps slightly decrease with the increase of the film thickness. Photoluminescence spectra of the thin films clearly show emission bands at about 1.63 and 2.32 eV at room temperature, with no shift observed with decreasing temperature. A model was proposed for explaining such anomaly.

Keywords: chalcogenides, thin films, optical properties, spectroscopy, SEM

I. Introduction

Selenides of copper (Cu-Se) exist in many phases and structural forms: i) stoichiometric forms, such as CuSe (klockmannite), Cu$_2$Se$_x$, CuSe$_2$ (marcasite), α-Cu$_2$Se (bellidoite), Cu$_3$Se$_2$ (umangite), Cu$_5$Se$_4$ (athabaskite), Cu$_7$Se$_4$ etc., as well as ii) non-stoichiometric forms, such as Cu$_{2-x}$Se (berzelianite). All those phases can be classified into several crystallographic forms (monoclinic, cubic, tetragonal, hexagonal, etc.). Copper selenide is a semiconductor with p-type conductivity, and has numerous applications in various devices, such as solar cells [1–3], photo detectors [4], optical filters [5], microwave shielding [6], thermoelectric converters [7], etc. Photovoltaic cells and Shottky diodes are also based on these metal chalcogenide compounds [8,9]. CuSe$_2$ is a superconductor at low temperatures with a transition temperature $T_C \sim 2.4$ K [10], and has a weak ferro-magnetic response below 31 K [11,12]. CuSe$_2$ is widely used as a precursor material for CuInSe$_2$ (CIS) and Cu(In,Ga)Se$_2$ (CIGS) preparation, suitable for highly efficient photovoltaic elements [13]. Also, CuSe$_2$ is used as a typical anion conductor and significant Cu-Se alloys targets for the preparation of CIGS/CIS thin film solar cells in RF magnetic sputtering [14].

Possible application of Cu-Se strongly depends on its optical properties. Despite the numerous publications of the optical properties of Cu-Se thin films, the estimated value of band gap of Cu-Se is not well defined. Cu-Se has both direct and indirect transitions, so the presence of both band gaps, direct and indirect, can be observed. Literature data are quite controversial: direct allowed transitions are reported to have corresponding band gap in the range of 2 to 3 eV, and indirect band gap between 1.1 and 1.5 eV [15–18]. The indirect band gap being near the optimum value for solar cell applications makes this material capable of potentially offer a high efficiency of conversion. However, Cu-Se nanoparticles

*Corresponding author: tel: +381 11 3713 036,
fax: +381 11 3713 052, e-mail: martina@ipb.ac.rs*

have been reported to possess a direct band gap of 4 eV and indirect one of 1.87 eV [19]. The reasons of such variation in band gaps could lie in the sharp cut off of the wavelength with the spectral transmittance instead of the slow increase, the presence of large number of dislocations, wide range of stoichiometric deviation and quantum confinement effect.

In our previous report [20], we prepared Cu-Se thin films of three different thicknesses by vacuum evaporation technique using Mo boat onto glass substrate at room temperature, and investigated their structural properties. XRD and far-infrared spectroscopy revealed the presence of $CuSe_2$ nanocrystals in predominant Se films.

The objective of this research was to determine optical properties of Cu-Se thin films, using UV-VIS and low-temperature photoluminescence spectroscopy, and to investigate how the film thickness could influence the band gap value and photoluminescence properties. SEM analysis was also performed in order to get information about the morphology of the obtained Cu-Se thin films.

II. Experimental

Thin films were obtained by evaporating commercially high purity CuSe powder (99.99%) supplied from Aldrich Company. The powder was deposited onto highly pre-cleaned glass substrates with use of Mo boat. The procedure was done in a high-vacuum environment with typical background pressures of 3 mPa. The deposition rate, 10 nm/s, was monitored by quartz crystal thickness monitor - FTM4, Edwards and the final films thicknesses was found to be 56 nm, 79 nm and 172 nm for the films labelled as F-55, F-80 and F-170, respectively [20].

SEM imaging was done using scanning electron microscope equipped with a high brightness Schottky field emission gun (FEGSEM, TESCAN) operating at 4 kV. The samples were coated with gold/palladium to make them conductive.

The UV-VIS diffusion reflectance and transmittance spectra were recorded in the wavelength range of 300–1000 nm on a Shimadzu UV-2600 spectrophotometer equipped with an integrated sphere. The diffuse reflectance and transmittance spectra were measured relative to a reference sample of $BaSO_4$.

Photoluminescence measurements on various temperatures ($T = 20$–300 K) were obtained by Jobin-Yvon U1000 spectrometer, equipped with RCA-C31034A photomultiplier with housing cooled by Peltier element, amplifiers and counters. The 488 nm laser line of argon laser was used as excitation source.

III. Results and discussion

3.1. SEM analyses

Scanning electron microscopy (SEM) images were obtained for the Cu-Se thin films deposited on glass substrate in order to study the surface morphology and
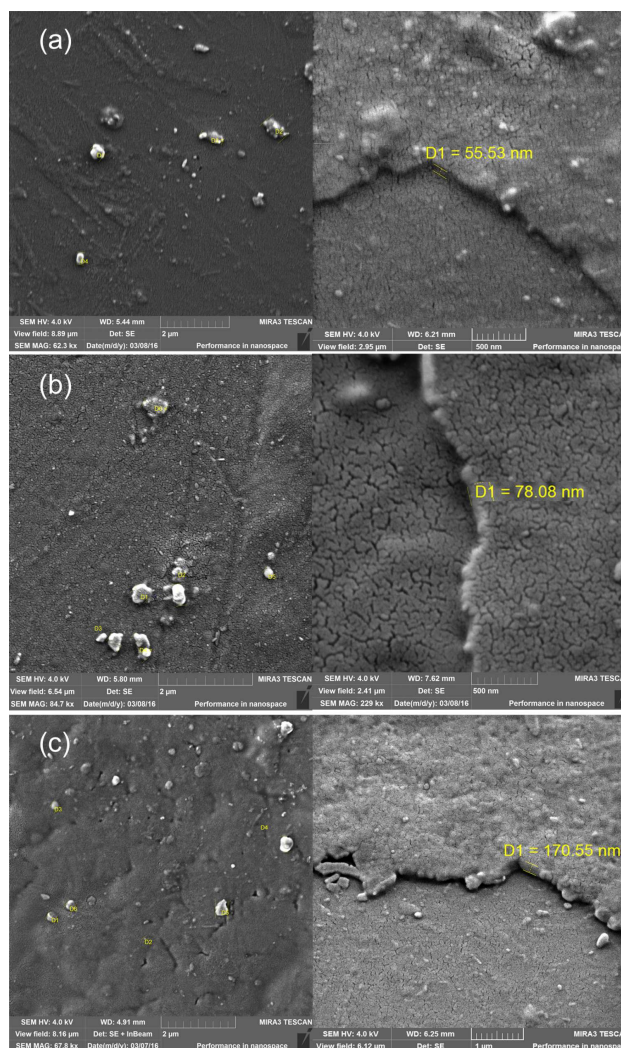

Figure 1. Top view and tilted SEM micrographs of films: a) F-55, b) F-80 and c) F-170

agglomeration of the samples.

Top view and tilted micrographs of the thin films are presented in Fig. 1. From the top view micrographs it can be observed that the surface of the samples is relatively uneven and rather rough, with presence of cracks and voids. Formation of the Cu-Se thin films most probably proceed unevenly, in the form of islands which later grew into agglomerates. Agglomerated clusters of few hundreds nanometers in diameter are distributed non-uniformly along the surface and form the structure consisting of $CuSe_2$ nanocrystals in predominant Se matrices. In order to determine the film thicknesses, the samples were tilted at 30°. The thicknesses estimated by SEM are: ~56 nm, ~78 nm and ~171 nm for the films F-55, F-80 and F-170, respectively. The thickness values estimated by SEM analysis match the ones obtained during the preparation of thin films.

3.2. UV-VIS spectroscopy

In Fig. 2 diffuse reflectance R and transmittance T spectra of the thin films samples in the wavelength range 300–1000 nm (4.13–1.24 eV) on room temperature (*T*
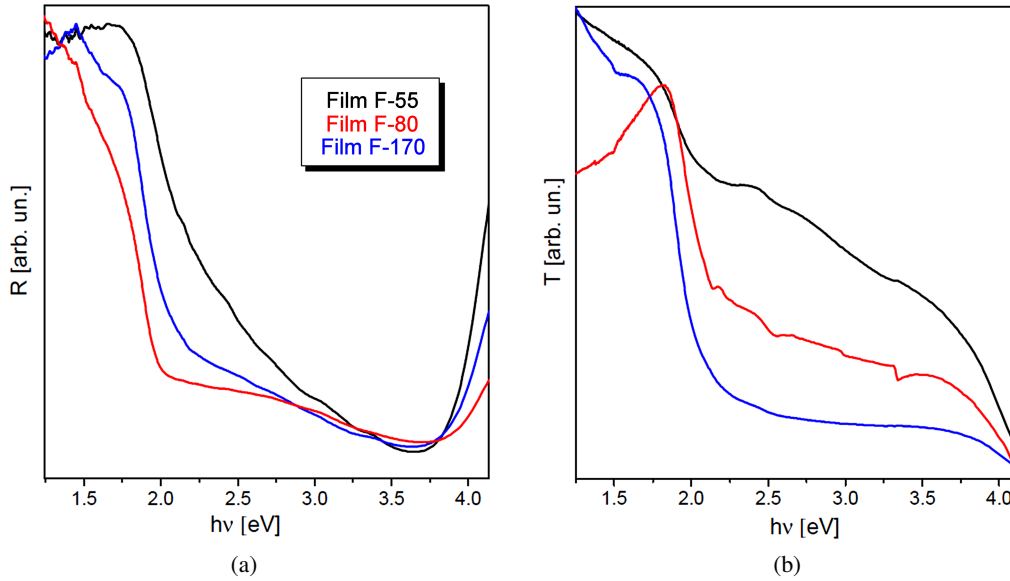
Figure 2. Diffuse reflectance, *R* (a), and transmittance, *T* (b) spectra

= 300 K) are presented. As it can be seen, the transmittance increases with decrease in the film thickness, which is not the case for reflectance. This is typical for films with high electrical conductivity and implies a reflection coefficient nearing 1 for films with metallic conductivity.

In this study we used the Tauc plot for the determination of the optical band gap from diffuse reflectance measurements. The determination of band gap in semiconductors is significant for obtaining the basic solid state physics. The relation expression proposed by Tauc, Davis and Mott [21–23] is the following:

$$\alpha \cdot h \cdot \nu = A \left(h \cdot \nu - E_g \right)^{1/n} \qquad (1)$$

where h is the Planck's constant, A is the transition probability constant depending on the effective mass of the charge carriers in the material, E_g is the band gap, $h \cdot \nu$ is the photon energy and α is the absorption coefficient which is defined as the relative rate of decrease in light intensity along its propagation path, i.e. a property of a material that defines the amount of light absorbed by it. The value of n denotes the nature of the transition. In case of direct transitions n equals ½ and 3⁄2 for allowed and forbidden transitions, respectively. As for indirect transitions, n equals 2 and 3 for allowed and forbidden transitions, respectively. Since CuSe exhibits both direct and indirect allowed transitions, n = ½ and n = 2.

Then, the acquired diffuse reflectance spectra are converted to Kubelka-Munk function [24]:

$$\alpha = \frac{(1-R)^2}{2R} \qquad (2)$$

So using this function, a plot of $(\alpha \cdot h \cdot \nu)^{1/n}$ against $h \cdot \nu$ is obtained. The energy band gap is determined by extrapolating the linear portion of $(\alpha \cdot h \cdot \nu)^{1/n}$ vs. $h \cdot \nu$

to the energy axis at $(\alpha \cdot h \cdot \nu)^{1/n} = 0$. The intercept of these plots on the energy axis gives the energy band gap. Such plots are given in Fig. 3. Direct transitions (left part of Fig. 3) reveal band gap for both selenium and CuSe$_2$, while indirect transitions (right part of Fig. 3) reveal band gap for CuSe$_2$ only.

The experimentally determined values of energy gaps for CuSe$_2$ show slight decrease with film thickness and their values range from 2.75 to 2.72 eV for direct transitions, and from 1.75 to 1.71 eV in case of indirect transitions. The estimated band gaps for selenium follow the same trend with film thickness and range between 2.33 and 2.36 eV. The estimated band gap positions for each sample are given in Table 1. The difference in the film thicknesses causes the small difference in band gaps in the second decimal place and they follow the well-established trend, the smaller the thickness, the wider the band gap is. Also, their values are quite wider than the ones that can be found in literature [7,16,25–33].

Table 1. Estimated band gap energies of thin films determined with UV-VIS spectroscopy

	F-55	F-80	F-170
CuSe$_2$ direct transition [eV]	2.75	2.74	2.72
CuSe$_2$ indirect transition [eV]	1.75	1.72	1.71
Se direct transition [eV]	2.36	2.34	2.33

Broad range of energy band gap values for Cu-Se can be found in literature. For direct transitions those values are usually between 2 and 3 eV. Bari *et al.* [25] obtained the value of 2.51 eV for the sample with thickness of 150 nm, and with the increase of film thickness they reported the decrease of band gap width. Grozdanov [26], Garcia *et al.* [16] and Sakr *et al.* [27] obtained the value of 2.33, 2.13–2.38 and 2.74 eV, respectively. The latter is very similar to the results obtained in this paper. Rajesh *et al.* [28] got a diversity of band gaps ranging from
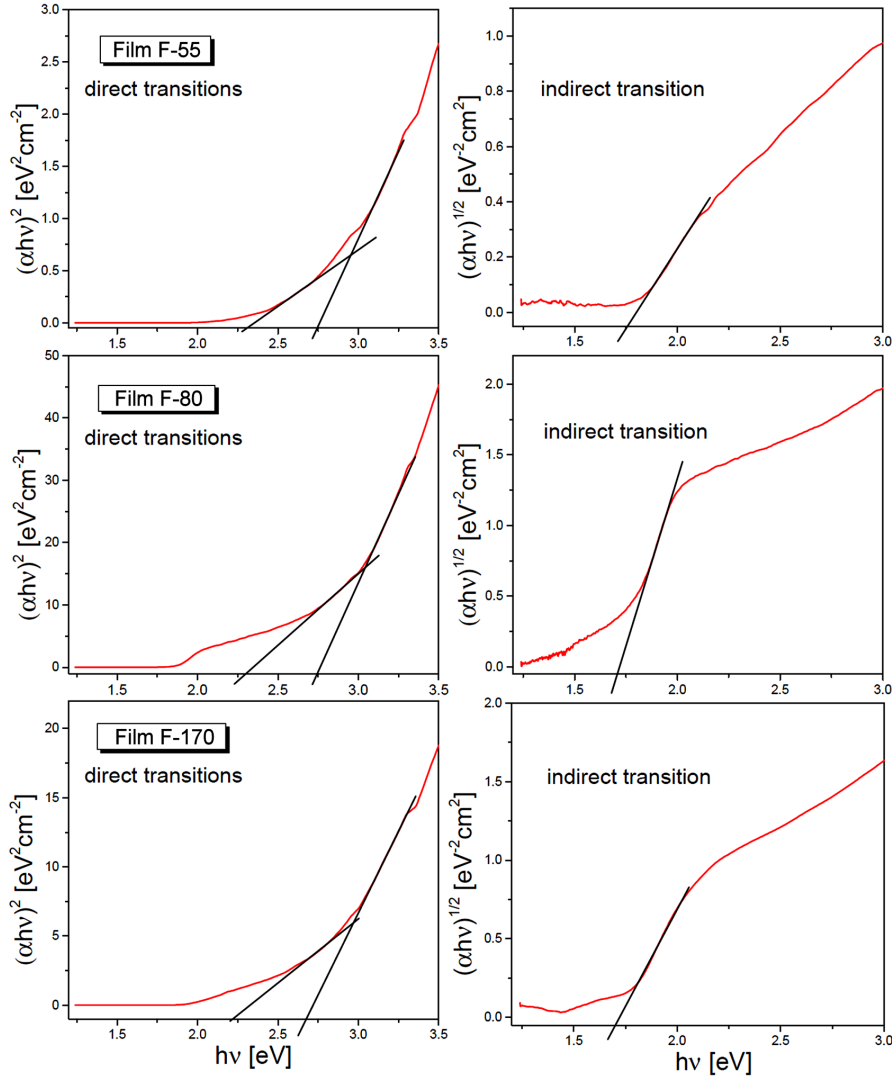
Figure 3. Dependence of $(\alpha \cdot h \cdot \nu)^2$ on photon energy $(h \cdot \nu)$ – left side, and dependence of $(\alpha \cdot h \cdot \nu)^{1/2}$ on photon energy $(h \cdot \nu)$ – right side

1.95 (the thickest film) to 3.70 eV (the thinnest film). However, for indirect transitions they received less attention. Garcia *et al.* [16] obtained values in the range 1.22–1.34 eV, whereas the value obtained by Bhuse *et al.* [7] is about 1.4 eV. Our values (~1.7 eV) are bigger than the reported in literature. According to our opinion, the larger indirect band gap values are due to quantum confinement effect [29,30] whereby the electrons are localized in individual crystallites, and due to specific border conditions between $CuSe_2$ nanoparticles and selenium matrix.

For the pure selenium, the direct band gap was reported to be about 2 eV for the bulk [31,32] and 2.20–2.06 for the thin films of thickness 130–290 nm [33]. Our films are thinner than the ones mentioned in the literature and it is not surprising that we obtained wider band gap values, about 2.3 eV. The film F-170 has the thickness between 130 and 290 nm, but the higher value in band gap is the result of specific border conditions between selenium matrix and $CuSe_2$ nanoparticles. We presume that $CuSe_2$ nanoparticles directly influence the

band gap of predominant selenium, and vice versa.

The Urbach energy is also analysed. Urbach rule states that the optical absorption coefficient α just below the band edge in insulators and semiconductors varies exponentially with the incident photon energy [34]:

$$\alpha = \alpha_0 \exp\left(\frac{h \cdot \nu}{E_U}\right) \qquad (3)$$

where α_0 is a constant and characteristic parameter of the material, $h \cdot \nu$ is incident photon energy, and the term E_U which is the width of the exponential tail is called Urbach energy. The Urbach energy represents the width of defect states in the band gap. Figure 4 shows $\log \alpha$ as a function of incident photon energy for the film F-170, as a representative one. By extrapolating the linear part of the plot and with use of Equation 3, the Urbach energy can be determined as the inverse of the slope and α_0 from the intercept of extrapolated plot. From the slope and inception of extrapolated plot it was determined that E_U is 0.32 eV and α_0 is 3.02 cm^{-1}.
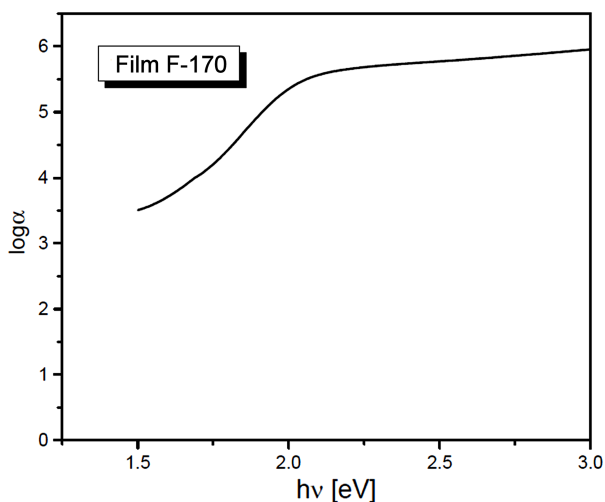
Figure 4. Logarithmic dependence of the absorption coefficient on the photon energy for F-170 film

3.3. Photoluminescence spectroscopy

Photoluminescence (PL) spectra can be used for investigating the possible outcomes of photo-induced electrons and holes in a semiconductor, since photoluminescence emission results from the recombination of free charge carriers. There are two types of photoluminescence phenomenon according to its attributes and formation mechanism: the band-to-band photoluminescence and the excitonic photoluminescence [35–37]. The band-to-band PL spectrum regards the separation situation of photo-generated charge carriers. The excitonic PL spectrum, however, cannot directly reflect the separation situation of photo-induced carriers. If discrete energy levels are present in the band gap, these may dominate the optical spectrum. PL measurements then yield information about the energetic positions of the electronic states in the gap. Such localized states can originate from various types of imperfections like vacancies, interstitial atoms, atoms at surfaces and grain boundaries. However, it is often difficult to determine the exact position and origin of these states.

Photoluminescence spectra of thin films on various temperatures are presented in Fig. 5. The spectra are rather complex, thus for their analysis the deconvolution method had to be employed. Two typical resolved spectra are presented in Fig. 6 (on 20 K and room temperature), and the deconvolution of the others is done in the same manner. Each spectrum is characterized with 5 bands. Band-to-band photoluminescence dominates the room temperature spectra. The band in red area at ~1.6 eV is clearly seen. According to the UV-VIS results (see previous chapter), we can attribute this mode to band-to-band transition for indirect transition in $CuSe_2$. In green area, a broad band is observed at ~2.3 eV which originates from direct transitions in selenium (also see prev. chapter). Due to Stokes shift, the obtained positions are a bit lower than the ones obtained by UV-VIS spectroscopy. Between these two bands there are three defect modes at 2.1 eV, 1.9 eV and
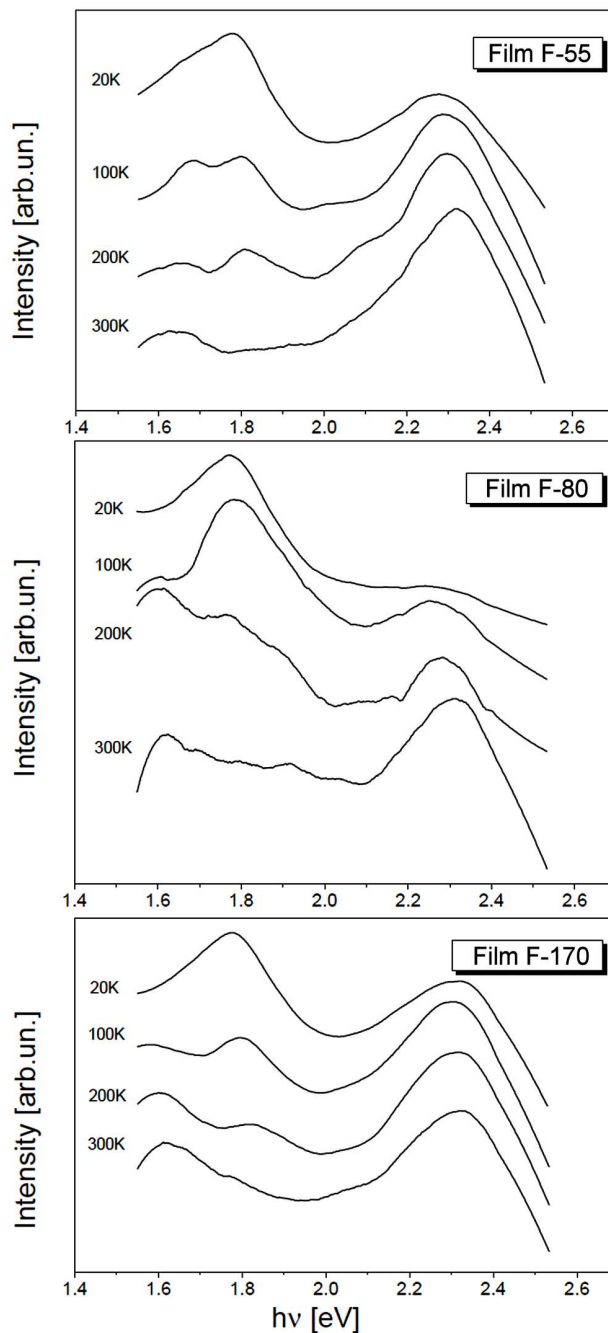

Figure 5. Photoluminescence spectra of thin films at various temperatures: a) F-55, b) F-80 and c) F-170

1.8 eV, which are of small intensity on room temperature. Lowering the temperature, the band at ~1.8 eV increases its intensity, and becomes the dominant one at 20 K. According to literature data [32] this band is attributed to selenium defect mode – negative U-centre. This mode is expected to appear at 0.5 eV from the band edges. Another two defect modes, at 2.1 and 1.9 eV, are attributed to the defect modes of $CuSe_2$, according to the work of Urmila *et al.* [38]. In their work they obtained bands at 2.1, 1.9 and 1.5 eV in PL spectrum of Cu_7Se_4 thin film. They concluded that there is nonradiative transition from conduction band to defect levels with energies 2.1, 1.9 and 1.5 eV and from these lev-
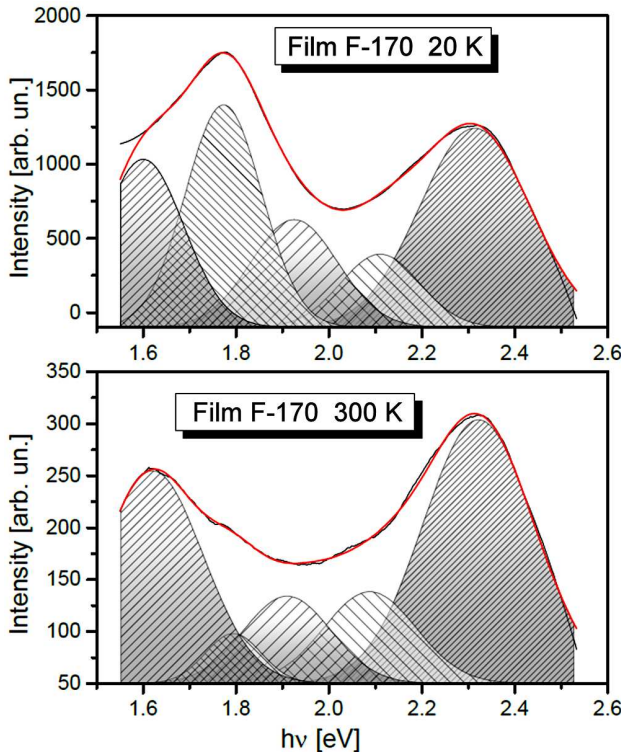
Figure 6. Typical resolved photoluminescence spectra of thin films F-170: a) on 20 K and b) room temperature
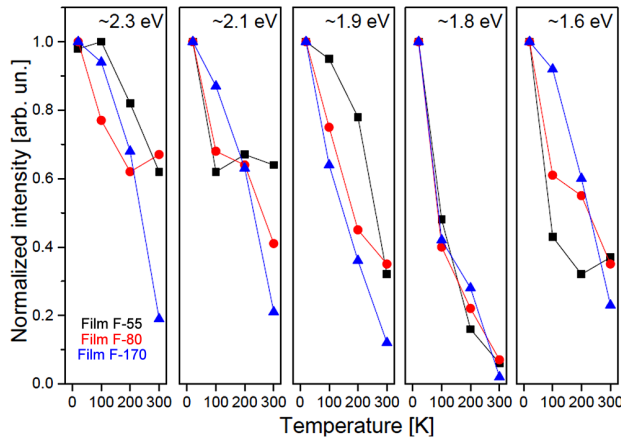

Figure 7. Temperature dependence of PL emission bands intensities, normalized on the most intensive ones (black squares – film F-55, red circles – film F-80, blue triangles – film F-170)

els radiative transitions occurred to valence band. The values 2.1 and 1.9 eV match the band positions we obtained in this work, thus we can assign these bands to defect modes in CuSe$_2$. Due to predominant phase of selenium, these bands are hidden by the bands originated from selenium and cannot be observed without the deconvolution method. Chong [39] in his work also obtained a PL band at ~2.16 eV without assigning it to any transition. In all spectra, the uprise of peak intensity with lowering temperature is observed, Fig. 7. The intensities have their maximum values at the lowest temperature (20 K) and show decrease with rising temperature. The most radical decrease is observed for the band

at ~1.8 eV, which intensity drops to ~40% at 200 K, and only to ~6% at room temperature.

Temperature dependence of PL emission band positions is shown in Fig. 8. Let us discuss the band position of indirect transitions of CuSe$_2$. At the room temperature, there are differences on the second decimal place for films of different thicknesses, the same as observed when analysing UV-VIS spectra. The same trend is observed on 20 K. If the shift of this band with temperature is analysed for each film, it can be noticed the temperature invariance, i.e. small non-monotonous differences in positions on the second decimal place. This is in contradiction with the expected red shift, characteristic for the semiconductors. The temperature invariance is observed for other bands as well. There is a question that needs to be answered: why the PL measurements show no shift with increasing temperature, instead of the conventional red shift characteristic for the semiconductors? A model proposed by Shen *et al.* [40] explains those discrepancies. It involves surface electron accumulation as a result of severe band bending in nanorods. However, the same trend was observed in thin film samples (including ours), whose curvature-less surface does not support a spatial charge separation such as in 1D nanostructures. Wei *et al.* [41] gave more exact explanation of this phenomenon in their work. They began the analysis by making difference between E_{PL} and E_g:

$$E_{PL}(n,T) = E_g(n,T) + E_{Fn}(n,T) - E_{Fp}(n,T) \quad (4)$$

where E_{Fn} and E_{Fp} are the electron and hole quasi-Fermi levels measured from the bottom of conduction band and the top of valence band, respectively. So the temperature dependence of the band gap shift is the competition between the lattice dilation dE_g/dT on the one hand, and the sum (dE_{Fn}/dT − dE_{Fp}/dT) on the other hand. The former results in the conventional red shift of the band gap with increasing temperature and the latter gets the blue shift. The resulting shift depends
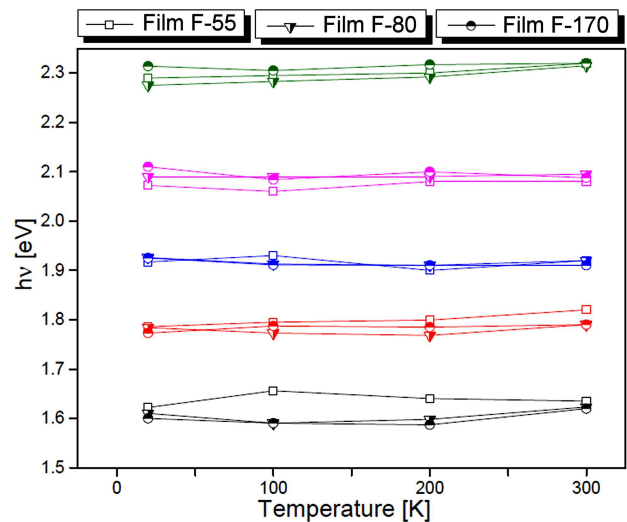

Figure 8. Temperature dependence of photoluminescence emission bands positions

on the magnitude of these two contributions. Usually when the electron density n is high, the thermal response in the material is governed by electronic rather than photonic interactions, the sum $(dE_{Fn}/dT - dE_{Fp}/dT)$ becomes dominant thus the blue shift of E_{PL} is observed. However, if these two contributions are of the same magnitude, it will result in no shift with changing temperature, as in case of our samples.

PL emission bands positions as a function of film thicknesses are presented in Fig. 9. It is common knowledge that as the confining dimension decreases, typically in nanoscale, the energy spectrum turns to discrete so the band gap of a semiconductor becomes size dependent. For one-dimensional confinement (film thickness), the quantization energies increase when the size along the confinement direction decreases [42,43]. In an amorphous or structurally disordered film, the imperfection in the film causes the bands of localized states to get broaden and a band gap reduction may occur due to the Urbach edge [44]. If we observe the shift of the band at ~1.6 eV, which corresponds to indirect transitions in $CuSe_2$, we can see the blue shift with decreasing size, as being expected. On the other hand, the band at ~2.3 eV which corresponds to direct transitions in Se, we can see no size dependence with the band position. The reason of this behaviour lies in specific composition of our films, i.e. $CuSe_2$ nano-objects embedded in selenium matrix. The particles of $CuSe_2$ are small enough to react on the size reduction, but the selenium matrix the amorphous effect becomes dominant.

As it can be seen from the above, the temperature changes do not affect the band gap. The size changes, i.e. the reduction of film thickness affects the band gap only on a second decimal place. Thus, we can state that the low cost technique of vacuum evaporation gives us the opportunity to produce quality, stable thin films
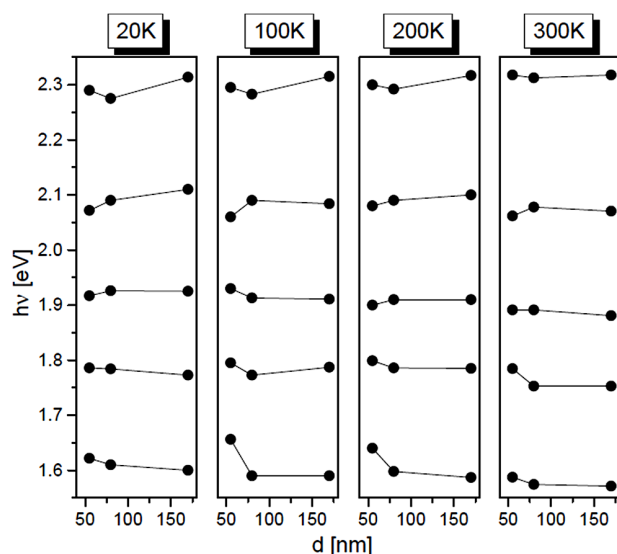
suitable for further applications in heterojunction solar cells and photo detectors.

IV. Conclusions

Cu-Se thin films of three different thicknesses, obtained by vacuum evaporation technique on glass substrate, underwent through photoluminescence investigation along with UV-VIS measurements and SEM analysis. Reflectance measurements revealed values for both direct and indirect band gap: ~2.7 and 1.7 eV, respectively for $CuSe_2$ and ~2.3 eV for Se. The existence of indirect band gap in $CuSe_2$ at this value, little wider than in literature, is confirmed by photoluminescence measurements. A band at ~1.8 eV, registered by PL measurements at low temperatures, is attributed to defect level of selenium – negative U-center. In this paper we proved that simple and low-cost technique as vacuum evaporation is capable of producing high-quality thin films.

References

1. T.P. Hsieh, C.C. Chuang, C.S. Wu, J.C. Chang, J.W. Guo, W.C. Chen, "Effects of residual copper selenide on CuInGaSe$_2$ solar cells", *Solid State Electron.*, **56** (2011) 175–178.
2. M. Singh, J. Jiu, T. Sugahara, K. Suganuma, "Thin-film copper indium gallium selenide solar cell based on low-temperature all-printing process", *ACS Appl. Mater. Interfaces*, **6** (2014) 16297–16303.
3. J.H. Scofield, A. Duda, D. Albin, B.L. Ballard, P.K. Predecki, "Sputtered molybdenum bilayer back contact for copper indium diselenide-based polycrystalline thin-film solar cells", *Thin Solid Films*, **260** (1995) 26–31.
4. S. Lei, A. Sobhani, F. Wen, A. George, Q. Wang, Y. Huang, P. Dong, B. Li, S. Najmaei, J. Bellah, G. Gupta, A.D. Mohite, L. Ge, J. Lou, N.J. Halas, R. Vajtai, P. Ajayan, "Ternary CuIn$_7$Se$_{11}$: Towards ultra-thin layered photodetectors and photovoltaic devices", *Adv. Mater.*, **45** (2014) 7666–7737.
5. G. Juska, V. Gulbinas, A. Jagminas, "Transient absorption of copper selenide nanowires of different stoichiometry", *Lith. J. Phys.*, **50** (2010) 233–239.
6. C. Levy-Clement, M. Neumann-Spallart, S.K. Haram, K.S.V. Santhanam, "Chemical bath deposition of cubic copper (I) selenide and its room temperature transformation to the orthorhombic phase", *Thin Solid Films*, **302** (1997) 12–16.
7. V.M. Bhuse, P.P. Hankare, K.M. Garadkar, A.S. Khomane, "A simple, convenient, low temperature route to grow polycrystalline copper selenide thin films", *Mater. Chem. Phys.*, **80** (2003) 82–88.
8. S.Y. Zhang, C. Fang, Y. Tian, K. Zhu, B. Jin, Y. Shen, J. Yang, "Synthesis and characterization of hexagonal CuSe nanotubes by templating against trigonal Se nanotubes", *Cryst. Growth Des.*, **6** (2006) 2809–2813.
9. H.M. Pathan, C.D. Lokhande, D.P. Amalnerkar, T. Seth, "Modified chemical deposition and physico-chemical

Figure 9. PL emission bands positions dependence of film thicknesses

properties of copper (I) selenide thin films", *Appl. Surf. Sci.*, **211** (2003) 48–56.

10. Y. Takana, N. Uchiyama, S. Ogawa, N. Mori, Y. Kimishima, S. Arisawa, A. Ishii, T. Hatano, K. Togano, "Superconducting properties of $CuS_{2-x}Se_x$ under high pressure", *Physica C: Superconduct.*, **341-348** (2000) 739–740.

11. G. Krill, P. Panissod, M.F. Lapierre, F. Gautier, C. Robert M.N. Eddine, "Magnetic properties and phase transitions of the metallic CuX_2 dichalogenides (X = S, Se, Te) with pyrite structure", *J. Phys. C*, **9** (1976) 1521–1533.

12. M. Kontani, T. Tutui, T. Moriwaka, T. Mizukoshi, "Specific heat and NMR studies on the pyrite-type superconductors CuS_2 and $CuSe_2$", *Physica B*, **284** (2000) 675–676.

13. R.R. Pai, T.T. John, M. Lakshimi, K.P. Vijayakumar, C.S. Kartha, "Observation of phase transitions in chemical bath deposited copper selenide thin films through conductivity studies", *Thin Solid Films*, **473** (2005) 208–212.

14. N.H. Kim, S. Oh, W.S. Lee, "Non-selenization method using sputtering deposition with a $CuSe_2$ target for CIGS thin film", *J. Korean Phys. Soc.*, **61** (2012) 1177–1180.

15. P. Hankare, A. Khomane, P. Chate, K. Rathod, K. Garadkar, "Preparation of copper selenide thin films by simple chemical route at low temperature and their characterization", *J. Alloys Comp.*, **469** (2009) 478–482.

16. V. Garcia, P. Nair, M. Nair, "Copper selenide thin films by chemical bath deposition", *J. Cryst. Growth*, **203** (1999) 113–124.

17. O. Arellano-Tanori, M. Acosta-Enriquez, R. Ochoa-Landin, R. Iniguez-Palomares, T. Mendivil-Reynoso, M. Flores-Acosta, S. Castillo, "Copper-selenide and copper-telluride composites powders sintetized by ionic exchange", *Chalcogenide Lett.*, **11** (2014) 13–19.

18. A. Jagminas, R. Juskenas, I. Gailiute, G. Statkute, R. Tomasinuas, "Electrochemical synthesis and optical characterization of copper selenide nanowire arrays within the alumina pores", *J. Cryst. Growth*, **294** (2006) 343–348.

19. D. Patidar, N.S. Saxena, "Characterization of single phase copper selenide nanoparticles and their growth mechanism", *J. Cryst. Growth*, **343** (2012) 68–72.

20. M. Gilic, M. Petrovic, R. Kostic, D. Stojanovic, T. Barudzija, M. Mitric, N. Romcevic, U. Ralevic, J. Trajic, M. Romcevic, I. Yahia, "Structural and optical properties of $CuSe_2$ nanocrystals formed in thin solid Cu-Se film", *Infrared Phys. Techn.*, **76** (2016) 276–284.

21. J. Tauc, R. Grigorovici, A. Vancu, "Optical properties and electronic structure of amorphous germanium", *Phys. Status Solidi*, **15** (1966) 627–637.

22. J. Tauc, *Optical Properties of Solids*, F. Abeles ed. North Holland, 1972.

23. E. Davis, N. Mott, "Conduction in non-crystalline systems V. Conductivity, optical absorption and photoconductivity in amorphous semiconductors", *Philos. Mag.*, **22** (1970) 903–922.

24. P. Kubelka, F. Munk, "Ein Beitrag zur Optik der Farbanstriche", *Zeits F. Teckn. Physik.*, **12** (1931) 593–601.

25. R. Bari, V. Ganesan, S. Potadar, L. Patil, "Structural, optical and electrical properties of chemically deposited copper selenide films", *Bull. Mater. Sci.*, **32** (2009) 37–42.

26. I. Grozdanov, "Electroconductive copper selenide films on transparent polyester sheets", *Synthetic Metals*, **63** (1994) 213–216.

27. G. Sakr, I. Yahia, M. Fadel, S. Fouad, N. Romcevic, "Optical spectroscopy, optical conductivity, dielectric properties and new methods for determining the gap states of CuSe thin films", *J. Alloys Comp.*, **507** (2010) 557–562.

28. D. Rajesh, R. Chandrakanth, C. Sunandana, "Annealing effects on the properties of copper selenide thin films for thermoelectric applications", *IOSR J. Appl. Phys.*, **4** (2013) 65–71.

29. G. Hodes, A. Albu-Yayor, F. Decker, P. Motisuke, "Three-dimensional quantum-size effect in chemically deposited cadmium selenide films", *Phys. Rev. B*, **36** (1987) 4215–4221.

30. V. García, M. Nair, P. Nair, R. Zingaro, "Chemical deposition of bismuth selenide thin films using N,N-dimethylselenourea", *Semicond. Sci. Technol.*, **12** (1997) 645–653.

31. S. Kasap, J.B. Frey, G. Belev, O. Tousignant, H. Mani, L. Laperriere, A. Reznik, J.A. Rowlands, "Amorphous selenium and its alloys from early xeroradiography to high resolution X-ray image detectors and ultrasensitive imaging tubes", *Phys. Status Solidi*, **246** (2009) 1794–1805.

32. M. Benkhedir, *Defect Levels in Amoprphous Selenium Bandgap*, Katholieke Universiteit Leuven, PhD Thesis 2006.

33. M. Singh, K. Bhahada, Y. Vijay, "Variation of optical band gap in obliquely deposited selenium thin films", *Indian J. Pure Appl. Phys.*, **43** (2005) 129–131.

34. F. Urbach, "The long-wavelength edge of photographic sensitivity and of the electronic absorption of solids", *Phys. Rev.*, **92** (1954) 1324.

35. F.B. Li, H.Z. Li, "Photocatalytic properties of gold/gold ion-modified titanium dioxide for wastewater treatment", *Appl. Catal. A*, **228** (2002) 15–27.

36. P. Kumar, K. Singh, "Wurtzite ZnSe quantum dots: Synthesis, characterization and PL properties", *J. Opto. Biomed. Mater.*, **1** (2009) 59–69.

37. J.G. Yu, Y.R. Su, B. Cheng, "Template-free fabrication and enhanced photocatalytic activity of hierarchical macro-/mesoporous titania", *Adv. Funct. Mater.*, **17** (2007) 1984–1990.

38. K. Urmila, N. Asokan, B. Pradeep, "Photoluminescence study of copper selenide thin films", *AIP Conf. Proc.*, **1391** (2011) 770–772.

39. W.S. Chong, "Synthesis and characterization of copper selenide nanoparticles via emulsion technique". *A project report submitted to the Department of Chemical Science Faculty of Science, Universiti Tunku Abdul Rahman*, In partial fulfilment of requirements for the degree of Bachelor of Science (Hons) Chemistry, May 2011.

40. C.H. Shen, H.Y. Chen, H.-W. Lin, S. Gwo, A.A. Klochikhin, V.Y. Davydov, "Near-infrared photoluminescence from vertical InN nanorod arrays grown on silicon: Effects of surface electron accumulation layer", *Appl. Phys. Lett.*, **88** (2006) 253104.

41. P. Wei, S. Chattopadhyay, F. Lin, C. Hsu, S. Jou, J. Chen, P. Huang, H. Hsu, H. Shih, K. Chen, L. Chen, "Origin of the anomalous temperature evolution of photoluminescence peak energy in degenerate InN nanocolumns", *Opt. Express*, **17** (2009) 11690–11697.

42. S.V. Gaponenko, *Optical Properties of Semiconductor Nanocrystals*, Cambridge University Press, Cambridge, 1998.

43. A. Shik, *Quantum Wells: Physics and Electronics of Two-*

Dimensional Systems, World Scientific, Singapore, 1997.

44. S.G. Tomlin, E. Khawaja, G.M.K. Thutupalli, "The optical properties of amorphous and crystalline germanium", *J. Phys. C*, **9** (1976) 4335–4347.